



**HAL**  
open science

## Surface treatments on commercial glasses: durable impact on the retention of lead, barium and boron

Léa Brunswic, Frederic Angeli, Stephane Gin, Eric van Hullebusch, Mariona Tarragó, Laurent Gautron, Daniel Neuville

### ► To cite this version:

Léa Brunswic, Frederic Angeli, Stephane Gin, Eric van Hullebusch, Mariona Tarragó, et al.. Surface treatments on commercial glasses: durable impact on the retention of lead, barium and boron. npj Materials Degradation, 2024, 8, pp.108. 10.1038/s41529-024-00526-x . cea-04766392

**HAL Id: cea-04766392**

**<https://cea.hal.science/cea-04766392v1>**

Submitted on 4 Nov 2024

**HAL** is a multi-disciplinary open access archive for the deposit and dissemination of scientific research documents, whether they are published or not. The documents may come from teaching and research institutions in France or abroad, or from public or private research centers.

L'archive ouverte pluridisciplinaire **HAL**, est destinée au dépôt et à la diffusion de documents scientifiques de niveau recherche, publiés ou non, émanant des établissements d'enseignement et de recherche français ou étrangers, des laboratoires publics ou privés.



Distributed under a Creative Commons Attribution 4.0 International License

<https://doi.org/10.1038/s41529-024-00526-x>

# Surface treatments on commercial glasses: durable impact on the retention of lead, barium and boron

Check for updates

L. Brunswic<sup>1</sup>, F. Angeli<sup>1</sup>✉, S. Gin<sup>1</sup>, E. D. van Hullebusch<sup>2</sup>, M. Tarrago<sup>2</sup>, L. Gautron<sup>3</sup> & D. R. Neuville<sup>2</sup>

Glass durability is one of the properties that can be affected by surface treatments such as coatings or chemical attacks. These treatments can be used to reduce the quantities of potentially toxic elements contained in glass that may be released in solution. Five surface treatments were selected: three different coatings (SnO<sub>2</sub>, TiO<sub>2</sub>, SiO<sub>2</sub>) and two acidic attacks (SO<sub>2</sub> dealkalization and acid polishing). These treatments were performed on five glass compositions (soda-lime, borosilicate, barium silicate, opal, and lead crystal). Their effects on alteration rates and mechanisms were investigated through a single protocol (acetic acid 4%, 70 °C) simulating accelerated aging conditions for containers of beverages or food. The data collected over 1.3 years showed significant reduction of lead leaching with all treatments except acid polishing. The best reduction factor was obtained with SO<sub>2</sub> dealkalization, which also demonstrated beneficial effects towards the retention of Ba by reducing the diffusion of alkalis.

The glass industry implements almost systematically surface coating strategies that offer tunable properties without modifying bulk glass composition nor melting processes. For instance, self-cleaning glasses for optics or the automotive industry are based on surface coatings reducing the visibility of fingerprints or preventing the sticking of dirt<sup>1</sup>. Alternatively, in heritage and conservation sciences Zn-based surface treatments were developed to protect ancient glasses from atmospheric alteration<sup>2</sup>. Indeed, glass durability is one of the properties that can be enhanced by surface treatments such as coatings or chemical modification of the surface. Both coatings and specific chemical attacks are of interest to reduce the alteration rate of a sustainable material like glass not only to improve its durability but also to comply with the regulations in force or to be enacted on glass. These latter especially impact the hollow glass industry to ensure the amounts of glass constituents leached by the glass items are absolutely harmless to consumers after extended use. In fact, some particular glass compositions contain high proportions of heavy metals like lead crystal glass, for instance, which must incorporate at least 24 wt% PbO to retain its designation<sup>3</sup>. Consequently, without surface treatment, after a long contact time, substantial quantities of lead can be released in crystal hollowware's content whether it is beverages, perfumes or edible goods<sup>4–11</sup>. Therefore lead is considered an element of concern, as well as boron, for which, some species, like boric acid (B<sub>2</sub>O<sub>3</sub>), was classified as carcinogenic, mutagenic and reprotoxic (CMR) by the CLP

regulation in Europe. Barium is also found in various quantities in soda-lime-based glasses and targeted by future regulation projects on food contact materials given its potential health impact<sup>12</sup>.

This work intends to compare the effects of surface treatments on glass alteration rates and mechanisms through a single protocol simulating accelerated aging conditions over long periods for containers of beverages or food. Therefore bestseller glass articles used daily by consumers were selected and treated with five different surface modifying treatments covering most of the application of glassware products and investigating over 25 combinations of glass with surface treatment. Each glass slab was treated and then altered in an inert container with acetic acid 4% vol. (pH = 2.4) in accordance with the standards on glass for food contact<sup>13</sup>, at 70 °C to fasten the alteration mechanisms for more than a year to mimic a worst-case scenario. The leaching solution were analysed by Inductively Coupled Plasma-Mass Spectrometry (ICP-MS) to measure the concentrations of glass constitutive elements leached out. The unique data collected gives access to quantitative information on more than 30 leaching tests yielding alteration behaviours spanning on duration exceeding by far any common test. The release of three elements of interest, lead, barium and boron was examined in depth because of their known or suspected hazardous effects for humans and/or the environment. Complementary approaches by Scanning Electron Microscopy (SEM) using Energy Dispersive

<sup>1</sup>CEA, DES, ISEC, DPME, Université de Montpellier, Marcoule, Bagnols-sur-Cèze Cedex, France. <sup>2</sup>Université Paris Cité, Institut de Physique du Globe de Paris, CNRS, Paris, France. <sup>3</sup>Laboratoire Géomatériaux et Environnement (LGE, EA 4508), Université Gustave Eiffel, Marne la Vallée Cedex 2, France.

✉ e-mail: [frederic.angeli@cea.fr](mailto:frederic.angeli@cea.fr)

Spectroscopy (EDS) and Time of Flight-Second Ion Mass Spectrometry (ToF-SIMS) were engaged to characterize samples before and after alteration at a micro to nanoscale. Thus, the changes in the distribution of elements between the underlying glass, the coating and the external medium were assessed.

## Results

Five silicate commercial glasses were investigated in this study covering a large array of glass compositions which are given in Table 1. In some cases, the exact composition of the glass cannot be divulged for industrial property reasons, but narrow composition ranges are provided. The chosen glass compositions are representative of different use of glass like tableware, cookware and containers in contact with food or cosmetic products. Glass A is often used to bottle spirituous beverages and corresponds to lead crystal glass. As such, glass A meets the criteria specified by the European Council Directive relating to crystal glass and contains 29 wt% PbO<sup>3</sup>. Glass B meets the requirement of the third crystal glass category described in the European Council Directive relating to crystal glass ( $\sum[\text{ZnO}, \text{BaO}, \text{PbO}, \text{K}_2\text{O}] \geq 10$  wt %). Glass B was developed as a lead-free alternative to lead crystal glass, integrating barium and is widely used for tableware. Soda-lime remains the most common glass used for packaging and is represented in our panel by glass C. Glass D is a borosilicate, also known as pyrex-type glass, famous for its heat resistance (until 300 °C) and widely used for oven dishes. The structure and durability of these glass compositions has been extensively studied in a previous work<sup>11</sup> with leaching experiments based on powder and carried out for 3 years under the same conditions of alteration. Glass O, correspond to opal crystallized glass, containing NaF, CaF<sub>2</sub> and BaF<sub>2</sub> crystals embedded in the glassy matrix and providing shock-resistant properties to this material.

Surface treatments used in the glass manufacturing industry were applied on these base glasses in industrial labs by industrial manufacturers. The selected surface treatments are of two kinds: acidic attacks of the glass surface or chemical deposits. The first category comprises two different processes both developed by the lead crystal glass industry: acid etching and surface dealkalinization. Acid etching is considered as one of the final steps of the lead crystal glass manufacturing process to give its shine to lead glass pieces. This step is mandatory to dissolve the most superficial microns of glass that were frosted during the cutting of decorating steps of the process, but yet the effect of this very aggressive treatment on lead crystal glass durability has not been reported to our knowledge, either for other glass

compositions. Surface dealkalinization was developed by crystal manufacturers to address the issue of lead migration from the containers to the contents outed in the 90's<sup>4,14,15</sup>. In the present study, samples were treated by SO<sub>2</sub> dealkalinization by two different manufacturers, each following their own trusted process and samples were labelled CEMa and CEMb, in reference to the vernacular name of this treatment known as cementation. A few scientific work have been published demonstrating the structural rearrangement of the dealkalinized glass impacting the surface properties of the material<sup>16</sup> as well as mechanical changes caused by SO<sub>2</sub> dealkalinization<sup>17,18</sup>. All these data demonstrated the increase of bridging oxygen (BO) at the surface of the glass.

The second category concerns coatings of different oxides deposited onto the glass surfaces which are designated as hot-end coatings in the glass industry. Silicon oxide deposit, SiO<sub>2</sub>, was developed to improve the mechanical surface properties of items on industrial conveying belts by modifying their surface tension. The targeted deposited thickness for this treatment was of 10 nm. Tin oxide deposit, SnO<sub>2</sub>, is one of the most widespread surface coating in the industry and can be found on the external surface of most glass items on the market. This treatment was originally meant to serve as a grip intermediate layer between glass and cold-end coatings often composed of organic compounds. Titanium oxide deposit, TiO<sub>2</sub> is used industrially to enhance the aesthetic properties of glass items but its effect on glass durability have not been tested nor published. Each combination of base glass and surface treatment was tested, as listed in Table 2, yielding a total of 30 different samples, to which a reference set of non-treated samples was added.

## Surface modifications induced by deposits and their chemical durability

**Tin oxide, dSn.** ToF-SIMS analyses were conducted on two pristine samples A\_dSn and C\_dSn as shown in Figs. 1, 2 and 3 to investigate the tin oxide layer. From the ToF-SIMS profiles of Sn on these 2 samples, the thickness of the tin oxide layer obtained was approximately of 7 nm for C\_dSn and 10 nm for A\_dSn. It is worth to note that the profiles were normalized to a mean rate of abrasion which does not take in consideration the difference of density between the surface tin oxide deposit and the underlying glass. Therefore the larger thickness observed on A\_dSn sample could be explained by the higher density of the underlying glass compared to glass C (the density of each glass is reported in Table 1) and cannot be considered as reflecting an absolute difference.

**Table 1 | Composition of the studied glasses analysed by ICP-AES after complete dissolution in acid (HF + HCl + HNO<sub>3</sub>), expressed in mol% and wt% of oxide alongside densities (SA/V = 2,5 cm<sup>-1</sup>, acetic acid 4%, pH = 2.4, 70 °C, 470 days)**

oxide	Glass A (Lead crystal)		Glass B (Barium glass)		Glass C (Soda-lime)		Glass D (Borosilicate)		Glass O (Opal)	
	mol%	wt%	mol%	wt%	mol%	wt%	mol%	wt%	mol%	wt%
SiO <sub>2</sub>	77.1	56.7	74.2	70.0	70.9	70.3	82.1	79.7	73.6	71.3
B <sub>2</sub> O <sub>3</sub>							10.7	12.0		
Na <sub>2</sub> O	0.8	0.6	8.3–10.3	8.0–10.3	13.0–15.0	13.0–15.0	5.6	5.6	11.9	12.0
Al <sub>2</sub> O <sub>3</sub>			<1.3	<2.0	<1.3	<2.0	1.6	2.6		
CaO			9.0–11.0	8.0–10.0	9.0–11.0	8.0–10.0			4.8	7.9
MgO					2.0–4.0	4.0			2.2	2.0
ZnO					0.2	0.3				
BaO			0.5–2.5	4.0–6.0	<1.0	<2.0			0.8	2.0
K <sub>2</sub> O	11.3	13.0	2.5–4.5	4.0–6.0	<1.0	<2.0			1.0	1.5
PbO	10.6	29.0								
Sb <sub>2</sub> O <sub>3</sub>	0.2	0.7								
SO <sub>2</sub>					0.1	0.1				
F <sub>2</sub>									5.7	3.5
Density (g/cm <sup>3</sup> )	3.03		2.57		2.52		2.27		2.41	

**Table 2 | Combinations of base glasses and surface treatments including chemical attacks or chemical deposits composing the samples studied**

Surface Glass	Ref	Treatments			Deposits		
		SO <sub>2</sub> dealcalization		Acid etching	SiO <sub>2</sub>	SnO <sub>2</sub>	TiO <sub>2</sub>
		CEMa	CEMb				
A, lead crystal	A	A_CEMa	A_CEMb	A_PA	A_dSi	A_dSn	A_dTi
B, barium cristalline	B	B_CEMa	B_CEMb	B_PA	B_dSi	B_dSn	B_dTi
C, soda-lime	C	C_CEMa	C_CEMb	C_PA	C_dSi	C_dSn	C_dTi
D, borosilicate	D	D_CEMa	D_CEMb	D_PA	D_dSi	D_dSn	D_dTi
O, crystallized opal	O	O_CEMa	O_CEMb	O_PA	O_dSi	O_dSn	O_dTi

A set of base glasses without surface treatments is included in the column 'Ref' for reference.

**Fig. 1 | ToF-SIMS profiles obtained from the analysis of the surfaces of glass C\_dSn before and after 112 days of alteration at 70 °C and pH = 2.4.** The results from the pristine glass are presented in (a, b) with solid lines. The yellow shaded area represents the depth occupied by the tin oxide coating. The results from the altered slab are presented in (c, d) with dashed lines. The signals are normalized to the total intensity and to the pristine glass signal, as described by Eq. (3).

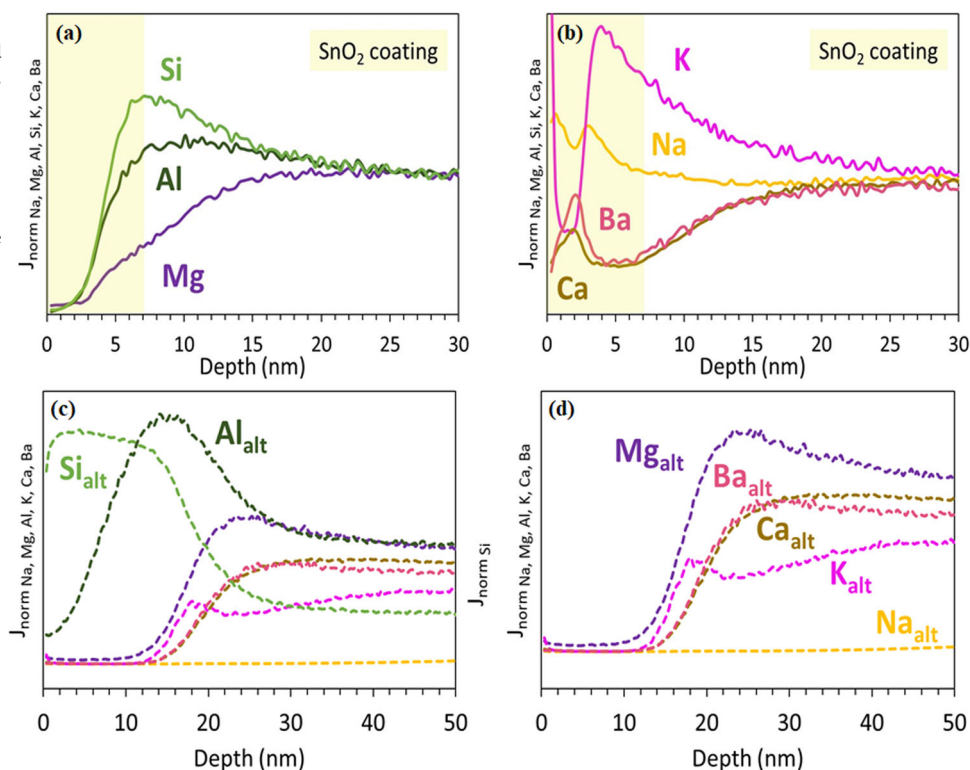
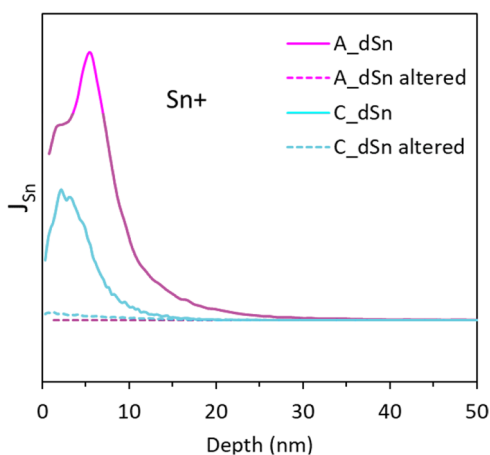
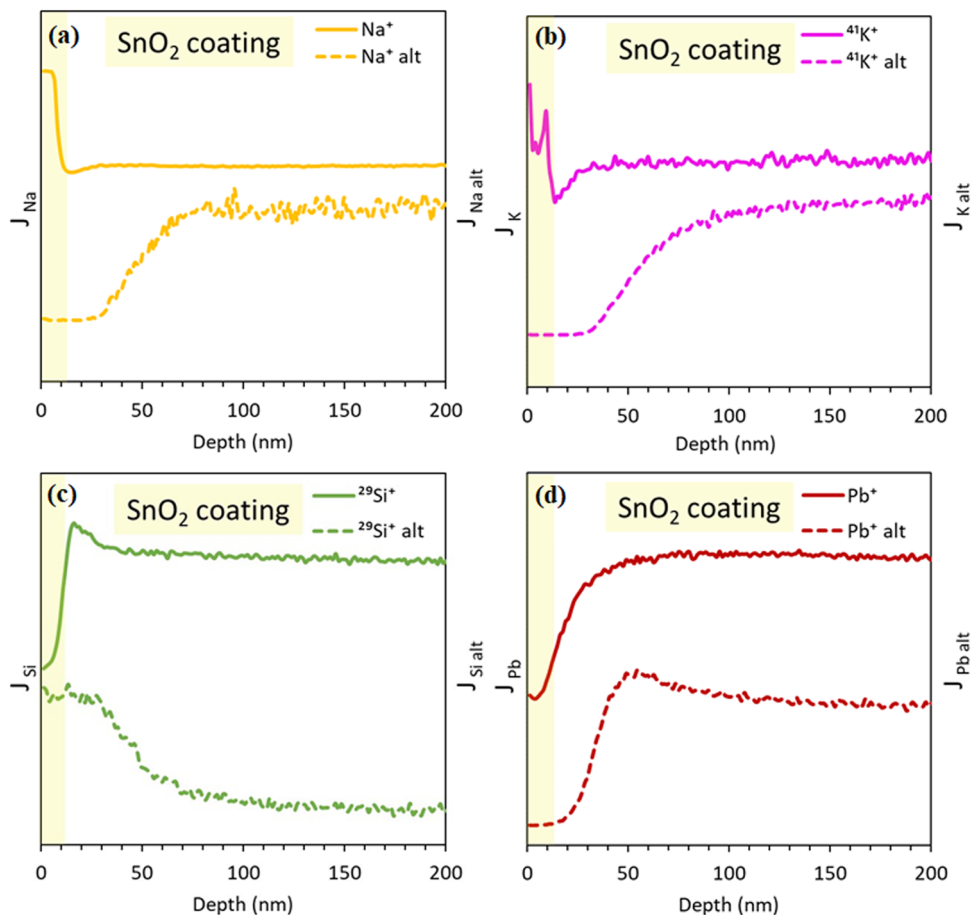


Figure 1a and b show the ToF-SIMS profiles of the major constituents of glass C\_dSn, unveiling the impacts of tin oxide deposit onto soda-lime pristine glass surfaces. Peculiar distributions of alkaline and earth-alkaline elements can be noticed in the topmost 5 nm of the sample, corresponding to the surface coating. Na, K, Ba and Ca (Fig. 1b) are found to migrate into the tin oxide deposit with different rates leading to the dwell of earth-alkaline Ca and Ba near the sample surface whereas Na and K seem to be positioned at the interface between the tin oxide coating and the underlying glass. Based on this observation, it can be inferred that the diffusion of these species was driven by their ionic charge rather than their size as Ca and Ba are larger but bearing two positive charges and diffused on longer distances compared to Na and K. Notably, Si, Al and Mg, which is also an earth-alkaline element, were not affected by the deposition of tin oxide and did not diffuse in the extreme surface layer. As a comparison, the effects of tin oxide on the surface of lead crystal glass (sample A\_dSn) constituting elements were examined by ToF-SIMS as well as discussed below. The results on pristine glass are shown with solid lines and confirmed the diffusion of alkaline species in the tin oxide coating as clearly observed by the accumulation of sodium and potassium in the uppermost 10 nm of glass A\_dSn shown in Fig. 2a and b

respectively. Tin oxide did not affect the distribution of Si nor Pb as evidenced by their ToF-SIMS profiles given in Fig. 2c and d. Overall, tin oxide coating on pristine glasses modified their most superficial composition through the diffusion of alkalis from the glass, as well as Ca and Ba if present, creating a layer of 10 nm at most, integrating elements from the glass to tin oxide.

Under the acidic, warm and very long alteration conditions applied, the tin oxide deposit did not resist. As shown by the ToF-SIMS profiles of Sn recorded after alteration on samples C\_dSn and A\_dSn and displayed with dashed lines in Fig. 3, the intensity of Sn was null and equivalent to the one recorded in the underlying glasses which did not contain Sn. A detailed view of the 50 first nm of glass C\_dSn after alteration is given in Fig. 1c and d while the profiles of all elements are given in Supplementary Fig. 1 showing a total remaining alteration layer of 300 nm. This layer is characterized by hydration correlated with Na depletion, archetypal of the ion-exchange mechanism of alteration. Over the inner 90% of this layer, all the constitutive glass elements but Na are retained. Nonetheless, K and Mg are depleted from the topmost 20 nm, slightly more retained than Ca and Ba, depleted over 25 nm, leaving a surface layer of 20 nm composed of hydrated silica in

**Fig. 2 | ToF-SIMS profiles obtained from the analysis of the surfaces of glass A\_dSn before (solid lines) and after 470 days of alteration (dashed lines) at 70 °C and pH = 2.4.** The comparison of results obtained for Na, K, Si, Pb are given in (a–d), respectively. The yellow shaded area represents the depth occupied by the tin oxide coating. The ions displayed represent the species detected by the mass spectrometer after sputtering and the signals are normalized to the total ion count as indicated by Eq. (2).



**Fig. 3 | ToF-SIMS profiles obtained for Sn from the analysis of the surfaces of glass C\_dSn before and after 112 days of alteration and glass A\_dSn before and after 470 days of alteration at 70 °C and pH = 2.4.** The results from the pristine glasses are presented with solid lines and the results from the altered slabs are presented with dashed lines. The ion displayed represents the species detected by the mass spectrometer after sputtering. The signals are normalized to the total ion count as indicated by Eq. (2).

its most external half and hydrated silica and aluminium in its inner half. The total depth of altered glass cannot be measured since the depth of hydrolysed glass, fully dissolved in solution, was not recorded. However, the rate of hydrolysis was much lower to the rate of ion exchange to enable the formation of a large remaining altered layer. All these observations are in

good agreement with the results obtained on the same soda-lime glass without tin oxide surface treatment altered under the same protocol of alteration for 231 days and published elsewhere<sup>11</sup>. Regarding lead crystal glass with tin oxide coating, A\_dSn, after 470 days, a remaining altered layer of nearly 10 μm depleted in alkalis was observed by SEM as illustrated below. The most superficial 200 nm of this layer was investigated by ToF-SIMS as reported with dashed lines in Fig. 2a–d highlighting a topmost layer of hydrated silica depleted in Pb and alkalis in accordance with previous data of lead crystal glass alteration reported in the literature<sup>10,11,19</sup>. As already observed for soda-lime glass, these notes on the alteration of lead crystal glass with tin oxide coating show no variation with the alteration of non-treated samples.

The extreme surface modifications observed on pristine treated glasses do not impact the long-term alteration of these glasses questioning the fate of tin oxide in the course of alteration. To answer this question the recording of Sn measured in solution by ICP-MS over time and normalized to the SA/V ratio ratio is presented in Fig. 4 for glasses A\_dSn, B\_dSn, D\_dSn and O\_dSn. The same behaviour is noticed for all the glasses investigated with the highest Sn concentrations recorded after 1 day of alteration, indicating the dissolution of the tin oxide coating within the first moments of alteration. A strong and rapid decrease of Sn concentration then occurred over the weeks suggesting the precipitation of tin or its adsorption onto the reactor’s surface although no precipitate was detected and no trace of Sn was found in the altered samples excluding its incorporation in the altered layers. The concentrations of Sn in solution were indeed very low, with  $1.07 \pm 0.06$  ppb of Sn per m<sup>2</sup> of glasses in solution at its most. Finally, the accumulated sodium observed by ToF-SIMS on the pristine glasses did not make a difference in the release of this element as shown in the plots of Na concentration normalized to SA/V given in Supplementary Fig. 2b, d, f, h, j.



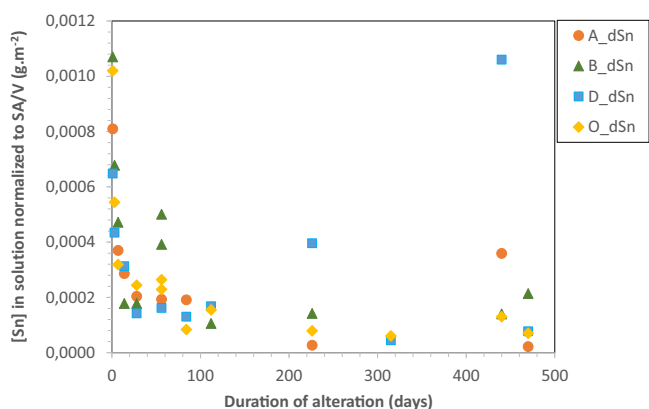


**Fig. 4 | Concentrations of Sn in solution normalized to the SA/V ratio for glasses with different tin oxide surface treatments.** Glasses A, B, D, and O are shown for Sn as a function of time (in days).

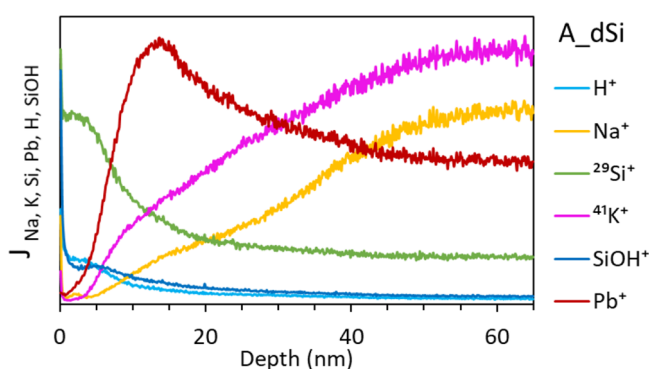


**Fig. 5 | ToF-SIMS profiles obtained on a pristine slab of A\_dSi, lead crystal glass with silicon deposit.** The ion displayed represent the species detected by the mass spectrometer after sputtering. The signals are normalized to the total ion count as indicated by Eq. (2).

**Silicon oxide, dSi.** Figure 5 displays the ToF-SIMS profiles obtained on the pristine surface of lead crystal glass with silicon oxide deposition, A\_dSi. As expected, Si is the only element detected within the topmost 10 nm of the glass exhibiting similar thicknesses for Si and Sn oxide deposits. But in contrast to the tin oxide treated samples, no diffusion of alkaline species from the glass into the silicon oxide was noticed. In fact, Na and K seem faded from the surface and gradually increase to stabilize only around 60 nm depth to their pristine glass level of intensity. Additionally, the recorded profiles of H<sup>+</sup> and SiOH<sup>+</sup> species indicate that, prior to alteration, the deposited silicon layer had a little higher level of hydration than the pristine underlying glass.

The comparison of Si released in solution by silicon oxide treated samples (A\_dSi, B\_dSi, C\_dSi, D\_dSi, O\_dSi) and reference glasses (with no surface treatment) is plotted in Fig. 6. For all the samples, the release of Si was mainly linear with respect to time, significant of a hydrolysis mechanism of alteration, with no difference induced by the silicon oxide surface coating. Apart from opal crystallized glass, O, the samples with silicon oxide surface deposit leach out more Si than their non-treated homologous, although the extend of this difference varied depending on the glass composition. Regarding sample O, opal crystallized glass, the leaching of Si from O\_dSi was lower than the one of non-coated sample O. Noticeably the leaching of Si from glass O was significantly higher than the ones found for the other glasses, and the leaching of O\_dSi was close to the leaching of glass C\_dSi indicating that there is a preferential release of Si from glass O compared to other glasses and this offset is corrected when silicon oxide surface coating is applied. The high alteration rate of glass O could be explained by the

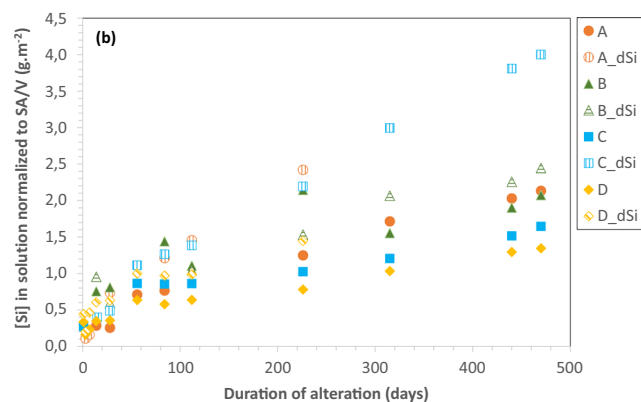
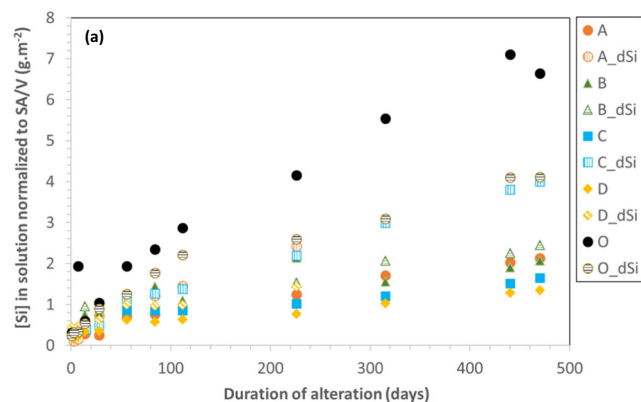


**Fig. 6 | Concentrations of Si in solution normalized to the SA/V ratio for glasses with different silicon surface treatment and reference glasses.** a all glasses, (b) glasses A, B, C, D.

accumulation of Na, Ca and Ba spreading over a few microns near the surfaces of the slab which occurs naturally during the manufacturing process of opal crystallized glass plates. Since no variation in the release of Si from coated samples after 470 days the durable effect of the silicon oxide coating can be underlined whether its impact is beneficial or detrimental compared to glasses with no surface treatment.

**Titanium oxide, dTi.** Since the titanium oxide coating was manually applied on the glass slabs, the obtained coating was not always homogeneous in terms of thickness and outcome. The variations of thickness were observed by SEM using a back-scattered electron detector sensitive to the atomic number which nicely allowed to distinguish the titanium oxide coating (lighter shades) from the glass (darker shades). The images are displayed in Fig. 7 showing local thicknesses ranging from 130 nm to over 500 nm depending on the spot of analysis. Furthermore, differences in morphology of the coating layer were noticed as reported in the SEM images with spherical appendices of titanium oxide coating forming at the surface of the glass. All these variations occurred at very local scales and were observed on all the different samples, regardless of the base glass.

A ToF-SIMS profile was run on the surface of A\_dTi pristine sample, but the depth of the crater could unfortunately not be measured because of the rugosity caused by the titanium oxide coating. The obtained results are therefore presented in Fig. 8 as a function of the sputtering time. Despite the very different properties of the coating and glass, these results show the diffusion of sodium across the at least 100 nm coating layer and its accumulation near the surface.

Regarding the durability of titanium oxide coating along the alteration process, the coated samples were observed by SEM with EDS mapping before and after 470 days of alteration, prepared as cross-sections. The

results are exposed in Fig. 9 where the signal of Ti was detected before as well as after alteration on all samples. Because of the high variations of titanium oxide thickness, it was not possible to determine precisely if there was a

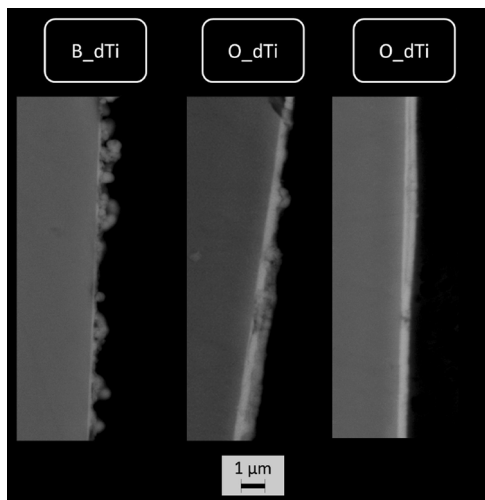


**Fig. 7 | SEM micrographs of pristine glass samples with titanium oxide coating prepared as polished cross-sections.** The images were acquired with back-scattered electron detector hence the lighter zones correspond to the titanium oxide deposit. Differences in terms of thickness and morphology are noticed among samples and within the same sample, like shown for O\_dTi.

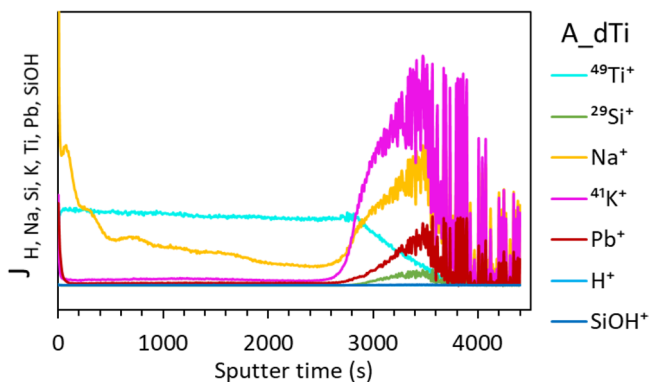
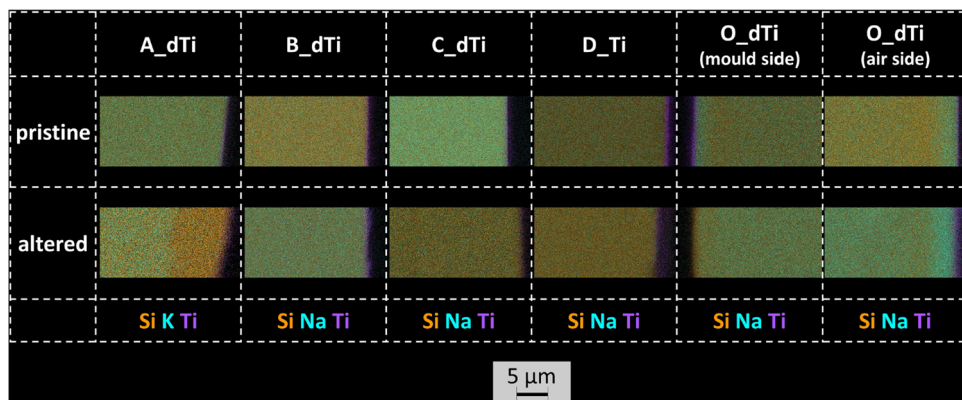


**Fig. 8 | ToF-SIMS profiles obtained on a pristine slab of A\_dTi, lead crystal glass with titanium oxide deposit.** The ion displayed represents the species detected by the mass spectrometer after sputtering. The signals are normalized to the total ion count as indicated by Eq. (2).

**Fig. 9 | SEM observations with chemical mapping by SEM-EDS of polished cross-sections of different base glasses (A, B, C, D and O) with surface treatment dTi (TiO<sub>2</sub> chemical deposit) before and after 470 days of alteration (acetic acid 4% vol., pH = 2.4, 70 °C).** For each sample, the original surface of the slab is on the right-hand side of the image and the bulk glass on the left-hand side.



change in the thickness of the remaining coating layer after alteration. Interestingly, the presence of the coating did not block the diffusion of elements from the underlying glass to the solution as evidenced by sample A\_dTi where a depleted layer in potassium of 7 µm is observed while the external titanium oxide layer is still detected. Nonetheless, the alkali-depleted layer measured on the reference sample of glass A without surface treatment was of 9.8 µm, as discussed further, suggesting a reduction of the rate of interdiffusion caused by the titanium surface coating. Additionally, titanium oxide coating showed interesting retention capacities towards elements like lead, barium or boron, as detailed in the further sections. That being, the measured concentrations of Si in solution of samples with and without titanium oxide surface coating were in the same range, as shown in Supplementary Fig. 2a, c, e, g, i.

The titanium concentration in solution was measured by ICP-MS over time then normalized to the SA/V ratio and the results are shown in Fig. 10. The absolute values of Ti found in solution range between 1 and 10 ppb per m<sup>2</sup> of glass exposed to solution, which remain very low, especially considering the important thickness of the coating thus confirming that most of the titanium oxide layer resisted to alteration and remained at the surface of the samples. Similarly to what was observed for Sn in the case of tin oxide-coated samples, Ti measured in solution strongly decreased over time suggesting the precipitation in the solution, which was not found or the adsorption of Ti. A dynamic mechanism with the continuous hydrolysis and precipitation of the tin oxide layer at the surface of the glass could explain its longevity but not in situ evidence of such a mechanism could be collected.

### Impact of surface treatments on the leaching of potentially hazardous elements

The impact of the investigated surface treatment was evaluated in light of the leaching of three critical elements: lead, barium and boron. For each of these elements, the comparison of the treated samples was carried out to determine the potential benefit of each treatment compared to the non-treated reference.

**Lead.** Surface treatments strongly impact the leaching of Pb from lead crystal glass in solution, as exhibited in Fig. 11. The substantial differences caused by the surface treatments applied are twofold: differences in terms of concentrations of Pb in solution and differences in terms of mechanism of alteration, both being interdependent. Regarding mechanisms of alteration, for glasses A\_PA, A\_dSi, A\_dSn and the non-treated reference A, the same pattern, already described in the literature<sup>10,11,19</sup> is observed with a strong release until 56 days of alteration followed by a durable plateau caused by the repolymerization of the silicate network, as well as a reorganization of the leached layer, forming a very efficient diffusive barrier effect towards Pb. Even though the mechanism for the release of Pb is the same, their efficiency towards the retention of Pb in solution varies, as stated in Fig. 11 and Table 3 which reports the concentration of Pb in solution after 1 day and the ratios of

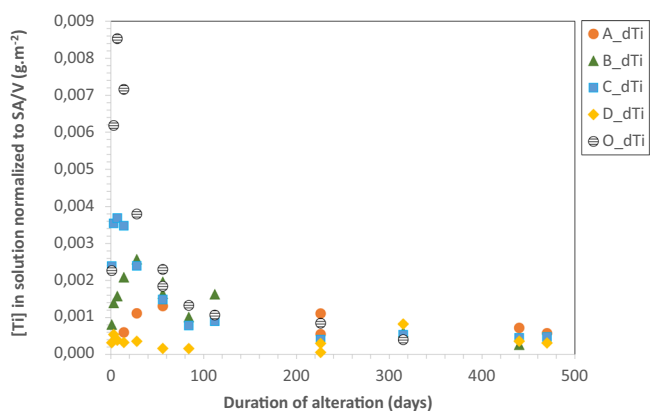


**Fig. 10 | Concentrations of Ti in solution normalized to the SA/V ratio for glasses with different titanium oxide surface treatments.** Glasses A, B, C, D, and O are shown for Ti as a function of time (in days).

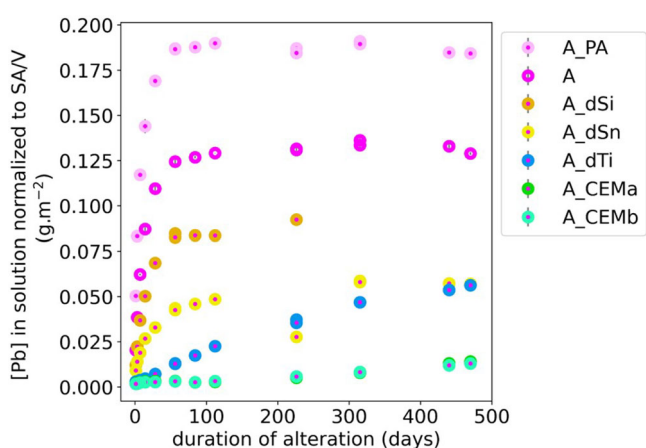


**Fig. 11 | Concentrations of Pb in solution normalized to SA/V for glasses A.** The various surface treatments were applied over 470 days of alteration (acetic acid 4% vol., pH = 2.4, 70 °C).

**Table 3 | Comparison of concentrations of Pb in solution after 470 days normalized to SA/V between glasses A with different surface treatments and a reference glass A without surface treatment**

Glass sample	[Pb] <sub>SA/V</sub> after 1 day g.m <sup>-2</sup>	[Pb] <sub>SA/V</sub> /[Pb] <sub>SA/V</sub> <sup>ref</sup>	
		1 day	470 days
A_PA	0.050	2.47	1.43
A (ref)	0.020	1.00	1.00
A_dSi	0.012	0.60	0.72 <sup>a</sup>
A_dSn	0.009	0.45	0.44
A_dTi	0.003	0.15	0.44
A_CEMa	0.002	0.09	0.11
A_CEMb	0.002	0.09	0.10

The relative uncertainty on these values is of 10%.  
<sup>a</sup>based on [Pb]<sub>SA/V</sub> at 226 days.

treated over non-treated concentration for each glass after 1 and 470 days of alteration. While A\_PA clearly increased the release of Pb, silicon oxide coating (A\_dSi) and tin oxide coating (A\_dSn) demonstrated interesting effect on the reduction of Pb release. Due to abnormal evaporation,

experiment on glass A\_dSi could not be carried out until 470 days and had to be stopped after 226 days, which was then considered to calculate the final [Pb]<sub>SA/V</sub>/[Pb]<sup>ref</sup> ratio stated in Table 3. The initial rate of alteration was determining for the retention capacity of Pb and a closer view of the first 60 days of alteration is given in Supplementary Fig. 3b. In contrast, the thickness of the remaining altered layer observed by SEM-EDS from polished cross-sections was very close for glasses A (non-treated), A\_PA, A\_dSi and A\_dSn, varying between 9.6 and 9.9 μm, as displayed in Fig. 12. All the layers were strongly depleted in alkalis, as expected and only K is shown because the weak proportion of Na in this glass does not allow to precisely map this element. Additionally, for samples A and A\_PA, a thin depleted layer in Pb can be noticed on the extreme surface of the samples, which is in good agreement with the leaching data. For a better estimation of the depleted layers in Pb, ToF-SIMS profiles were conducted on these samples before and after alteration. The results are given in Fig. 13a for glass A\_PA and Fig. 13b for glasses A\_dSn and A\_dSi. A remaining depleted layer of 170 nm was recorded for glass A\_PA and 50 nm only for glass A\_dSn, which is consistent with the trend obtained from the analyses of the leaching solutions. From these results, it can be deduced that the depleted layer in alkalis observed by SEM and constituting the majority of the altered layer is not proportional to the depleted layer in Pb. Overall, acid etching, tin oxide coating and silicon oxide coating do not have an impact on the nature of the alteration mechanisms nor on the leaching of alkalis. However, their influence on the kinetics of release of Pb is not negligible and the rate of alteration is determined to evaluate the long-term capacity of treated glass to retain efficiently Pb.

Considering sample A\_dTi, the release of Pb appeared linear over time, testifying of a different alteration/retention mechanism, potentially based on the hydrolysis of the coated glass. Because of this difference, titanium oxide coating showed more interesting properties on the shorter run than on the longer run compared to other coatings. The examination of sample A\_dTi after 470 days by SEM-EDX (Fig. 12) showed the presence of titanium at the surface of the slab indicating the strong resistance of this coating to acidic and long-term alteration. Below the residual titanium oxide coating, an alkali-depleted layer of 7 μm was observed confirming that ion-exchange mechanism is not inhibited by the coating, although the thickness of the alkali-depleted layer on the non-treated sample was of 9.8 μm suggesting that the coating partially inhibited or slowed down the rate of diffusion. Regarding Pb, the awaited thickness suggested by the analyses of the alteration solution (Fig. 11) would not be detectable through SEM and no depleted layer in Pb was observed. Moreover, our mappings were not precise enough to detect diffusion of Pb or other constitutive glass elements across the titanium oxide remaining coating. SO<sub>2</sub> dealkalinization treatments performed on samples A\_CEMa and A\_CEMb show particularly low amounts of Pb released compared to reference non-treated glass and other treated samples.

A detailed view of the leaching plot between 0 and 0.015 g.m<sup>-2</sup> is given in Supplementary Fig. 3a. The mechanism of alteration involved seems to be combining the classical mechanism observed for non-treated lead crystal glass followed by the a behaviour resembling the observations made for sample A\_dTi. Until a hundred days, the behaviour observed for the leaching of Pb from SO<sub>2</sub> dealkalinized samples showed an initial release and a plateau, although at a much lower scale than observed for a non-treated sample but after a hundred days the alteration rate resumed and showed linear dependency towards time. Since no difference was noted between samples A\_CEMa and A\_CEMb, the SEM-EDX mapping of sample A\_CEMb only was carried out and the result is given in Fig. 12. Standing out from all the other observations, no remaining altered layer was detected using SEM microscopy. This observation indicates that the ion-exchange rate for this glass cannot be higher than the rate of hydrolysis, which must be low considering the very small amounts of Pb as well as Na (shown in Supplementary Fig. 2b) measured for this glass. The precise depleted depth of Pb was measured by ToF-SIMS before and after alteration for A\_CEMa and A\_CEMb samples as shown in Fig. 13c. The



**Fig. 12 | SEM observations with chemical mapping by SEM-EDS of polished cross-sections of glasses A with different surface treatments after 470 days of alteration (acetic acid 4% vol., pH = 2.4, 70 °C). For each sample, the original surface of the slab is on the right-hand side of the image and the bulk glass on the left-hand side. The position and thickness of the remaining altered layers detected are indicated below each image.**

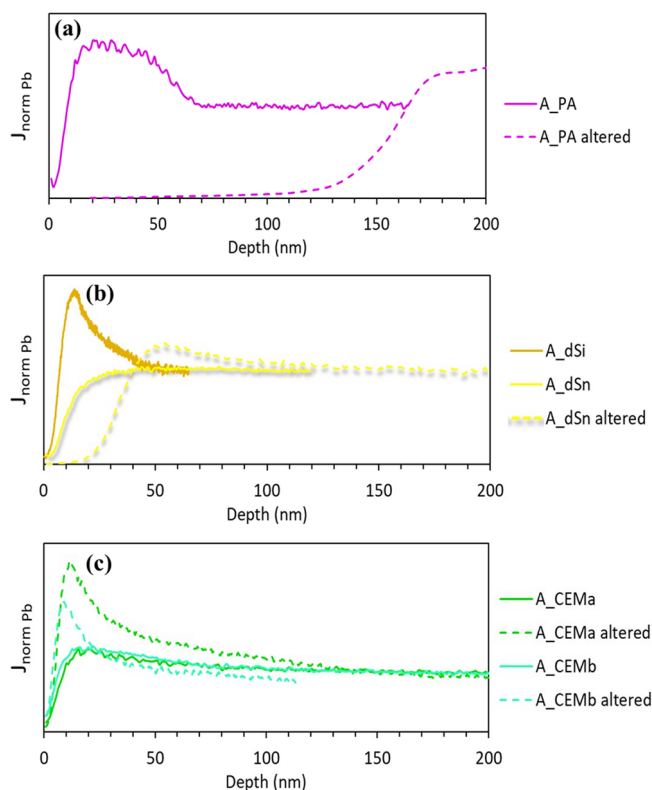
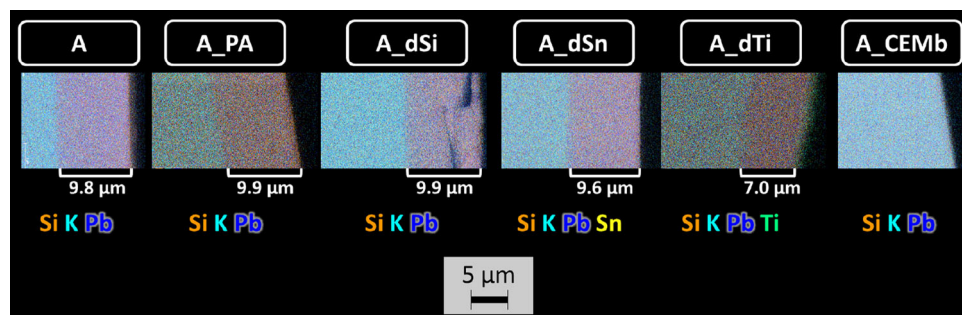


**Fig. 13 | ToF-SIMS profiles obtained for Pb from the analysis of pristine and altered slabs of glass A with different surface treatment.** The treatments are A\_PA (a), A\_dSi and A\_dSn (b) and A\_CEMa and A\_CEMb (c). The results from the pristine slabs are presented with solid lines and the results from the altered slabs are presented with dashed lines. The signals are normalized to the total intensity and to the pristine glass signal, as described by Eq. (3).

results obtained for both glasses are the same establishing that a 15 nm depleted layer in Pb at the surface of treated samples before and after alteration, supporting the idea of a hydrolysis mechanism governing alteration on the long term. The very low initial alkali content of these glasses caused by the surface treatment strongly slowed down the ion-exchange rate, which is responsible for the low Pb release observed between 0 and 100 days of alteration and then dominated by the rate of hydrolysis of the altered glass during the rest of the experiment.

**Barium.** Glass B has more barium in its initial composition than glass C, as stated in Table 1, which is reflected in the concentrations of Ba measured in solution during the alteration of glass B and C with different surface treatment. Figures 14a and b report the evolution of Ba in solution for the samples based on glass B and C, respectively, and the conclusions are similar: tin oxide and silicon oxide surface coatings as well as acid

etching do not affect the leaching of barium which remained very similar to the leaching of the reference non-treated samples. Whereas  $\text{SO}_2$  dealkalinization, (B\_CEMa, B\_CEMb, C\_CEMa, C\_CEMb samples) and titanium oxide coating (B\_dTi and C\_dTi samples) show interesting lowering properties towards Ba leaching, dividing 5 times the concentration of Ba in solution after 470 days of alteration compared to non-treated glasses. The observation of all the altered samples from glass B and glass C by SEM microscopy disclosed only residual titanium oxide coating at the surface of B\_dTi and C\_dTi altered samples as presented in Fig. 9 but no remaining altered layers were observed. Subsequently, it can be assumed that these remaining altered layers were thinner than 500 nm or very poorly depleted. Therefore ToF-SIMS was employed to analyse samples B\_CEMb and C\_CEMb before and after alteration. The results are given in Fig. 15 and brought out differences between both glasses. For B\_CEMb sample, the depth in Ba depleted are very similar before and after alteration, establishing that Ba is released by hydrolysis of the surrounding silicate network, in good agreement with the solution analyses showing linear release over time. For glass C, the difference between profiles before and after alteration is more substantial with an increase of the depleted depth of Ba in link with the alteration process. From the concentrations of Ba in solution, it can be noticed that after 300 days of alteration the leaching of Ba increased, explaining the larger depleted depth recorded by ToF-SIMS.

Geochemical tests were conducted using Chess (Thermochimiev9 database) and the PHREEQC database, considering the most concentrated solutions from the experiments. Under the temperature and pH conditions of these experiments, the solutions are both significantly undersaturated with respect to the secondary phases available in the databases for Ba. The same observation is made on the previous results with Pb.

The surface of glass O is characterized by a fully vitreous material with an accumulation of sodium, barium and calcium in the micrometre scale near the surface at the pristine state. This accumulation is responsible for the high release of Ba noticed in solution from non-treated glass O in Fig. 14c, which has an average BaO content of 0.8 wt% but released more Ba than glass sample B, which has 4–6 wt% of BaO. Additionally, the release of Ba from glass O was not linear in function of time but showed a strong initial release rate between 0 and 56 days of alteration followed by a drop of this rate typical of an ion-exchange mechanism and accentuated by the natural decreasing gradient of concentration of Ba between the surface and the bulk of the slab. Regarding silicon oxide and tin oxide coatings, no variation in the mechanism of alteration nor concentration of Ba in solution is noticed compared to non-treated glass O reference. For titanium oxide coating, a strictly linear release of Ba is noticed, indicating that the hydrolysis of the surrounding silicate network is driven the release of Ba in this sample at a constant rate. The same mechanism was noticed for Ba in samples B\_dTi and C\_Ti although the difference between concentrations in Ba from non-treated samples and titanium oxide-coated samples was greater after 470 days of alteration. In the case of glass O, after 470 days of alteration, the concentrations of Ba in solution from non-treated sample O and O\_dTi are very similar, which decreases the interest of this surface treatment over time. For  $\text{SO}_2$  dealkalinized samples, O\_CEMa and O\_CEMb, a strong decrease of

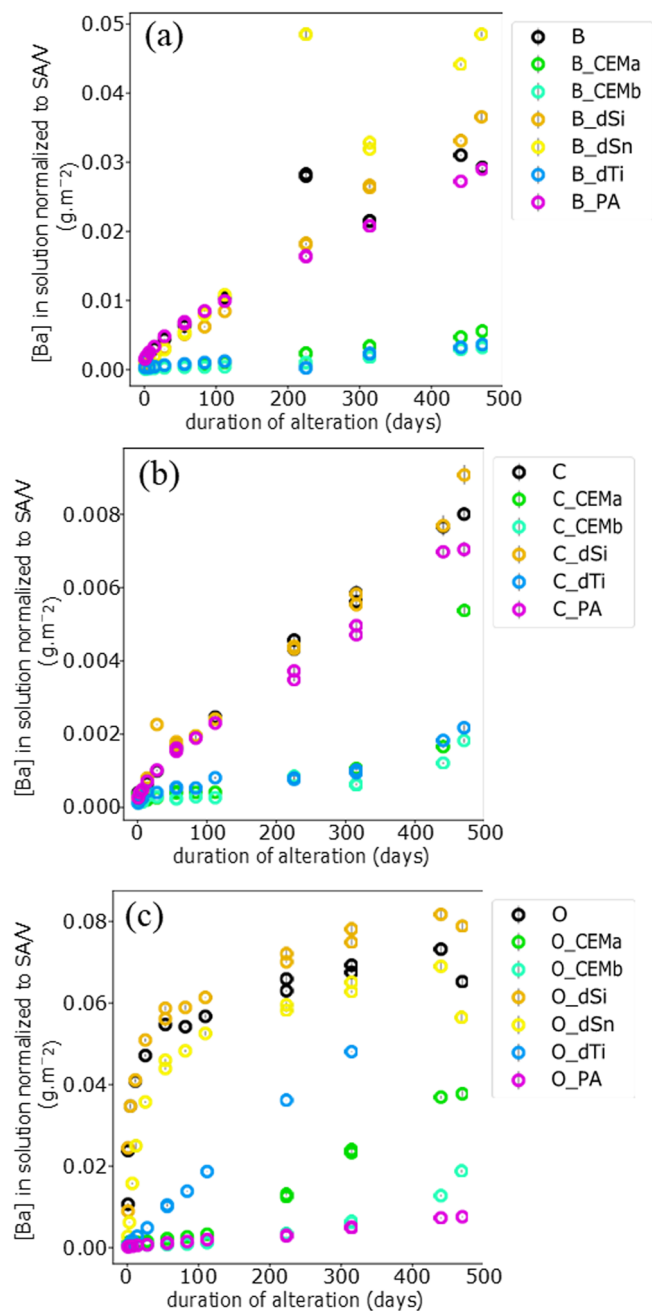


**Fig. 14 | Concentrations of Ba in solution normalized to the SA/V ratio.** Glasses B (a), C (b), and O (c) are shown for Ba as a function of time (in days) with the various surface treatments.

the release of Ba in solution is noticed as well a hydrolysis-driven mechanism of alteration until 112 days of alteration. After 112 days, a higher release rate of Ba is noticed for O\_CEMa compared to O\_CEMb suggesting different efficiency of the SO<sub>2</sub> vapour treatment on glass O. But the most effective surface treatment with glass O for the long-term retention of Ba is acid etching as shown by the release of Ba measured for glass O\_PA. Acid etching is a highly abrasive process greatly modifies glass surfaces. In the case of glass O, several microns of glass were dissolved which strongly impacted the structure of the air side of the slab. Consequently, the crystal-free first microns enriched in Na, Ba were removed and a new surface was disclosed. This new surface was constituted of crystals embedded in the glassy matrix with no gradient of Na, Ba or Ca, as shown in the SEM images of the pristine O\_PA glass slab displayed in Supplementary Fig. 4. The presence of

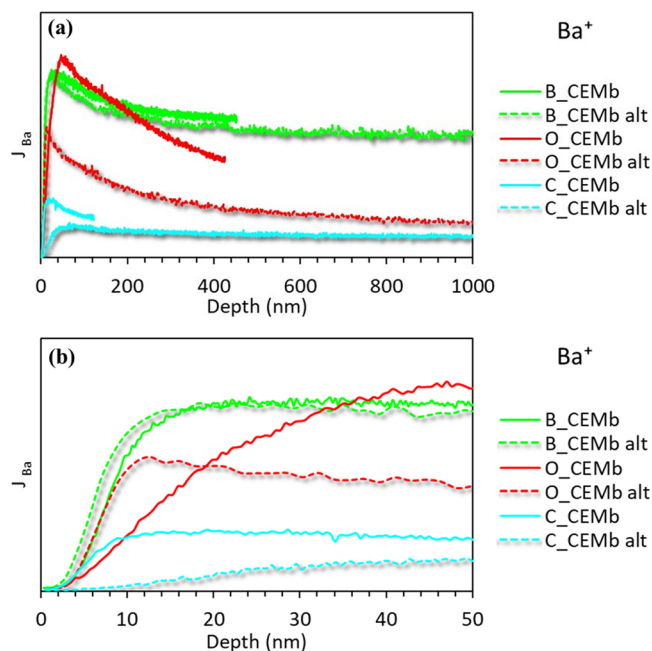


**Fig. 15 | ToF-SIMS profiles obtained for barium from pristine and altered SO<sub>2</sub> dealkalized samples of glass B (B\_CEMb), C (C\_CEMb) and O (O\_CEMb).** The results from the pristine slabs are presented with solid lines and the results from the altered slabs are presented with dashed lines. **b** Is a zoom on the superficial region of (a). The signals are normalized to the total intensity and to the pristine glass signal, as described by Eq. (3).

crystalline phases together with a homogeneous vitreous matrix without gradient at the surface of the slab increased the durability of the glass, hence a higher retention of Ba for O\_PA sample.

**Boron.** In Europe, since 2021 boron is subjected to more restrictive regulations because of the carcinogenicity of certain boron compounds<sup>20</sup>. Consequently, the release of boron from borosilicate glasses is scrutinized and the concentrations in this element found in solution for non-treated and treated borosilicate glass samples are given in Fig. 16. For non-treated glass sample, D, the release of boron was linear with respect to time as awaited from the structure and durability of this glass, which has already been described elsewhere<sup>11,21</sup>. Additionally, the alteration of this glass was demonstrated to be driven by the hydrolysis of the silicate network<sup>11,22</sup>, hence the linear release of B. For treated samples with tin oxide and silicon oxide coatings (D\_dSn and D\_dSi), no differences with the non-treated glass sample were observed, hence a nonexistent impact of these treatments on the mechanisms nor extend of the leaching of boron. For D\_PA, the release of boron was higher than for the non-treated sample with an important initial rate between 0 and 56 days followed by a slight drop which might be indicative of a retention mechanism of boron. In this case, the surface modification caused by acid etching may have depolymerized the silicate network and thus weakened the surface silicate network causing a higher leaching rate. SO<sub>2</sub> dealkalization treatments have shown distinctive responses in terms of B release, as observed from the differences noticed between samples D\_CEMa and D\_CEMb in Fig. 16. This discrepancy might occur from the different treatment processes but most significantly showed the non-relevance of SO<sub>2</sub> dealkalization treatments for congruently altered glasses which are driven by their rate of hydrolysis which did not seem impacted.

Finally, the most efficient surface treatment for boron retention was titanium oxide coating, which divided by 3 the concentrations of B in solution after 470 days compared to non-treated samples. However, the release of B from D\_dTi sample was not linear but exhibited an initial phase of release between 0 and 56, then followed by a sharp drop of alteration lasting over time.

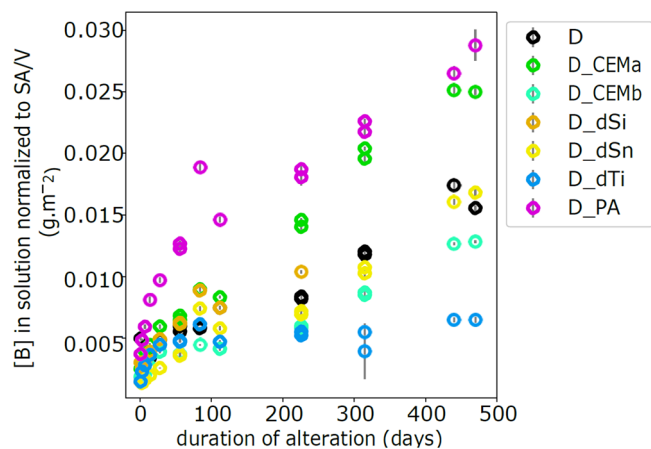


**Fig. 16 | Concentrations of B in solution normalized to the SA/V ratio.** Glasses D is shown for B as a function of time (in days) with the various surface treatments.

## Discussion

The alteration of glass compositions representative of the current consumer market with different industrial surface treatments was reported in this extensive study under conditions allowing direct comparisons. At a very local scale, the migration of alkalis into thin deposited surface coatings (<50 nm) induced by surface coatings themselves was observed with weak impact on long-term alteration. Surface treatments that significantly reduce the leaching of critical elements are those that strongly dealkalize the surface before alteration, preventing ion exchange and interdiffusion mechanisms during alteration, and demonstrating effectiveness for over a year. In the case of tin oxide coating, no measurable impact on long-term alteration was noticed given the very thin thickness of materials modified (<10 nm) and its rapid dissolution in contact with the alteration solution. For a silicon oxide coating of the same thickness, a long-lasting impact on the release of Si was acknowledged although not always favourable to glass durability. Titanium oxide coating of several hundreds of nanometres has proven its barrier effect over time regarding different elements due to its high thickness.

A part of lead crystal glass hollowware available for purchase is treated by SO<sub>2</sub> dealkalization, confirming the ubiquity of surface treatments in the glass industry and in consumers' daily life. From past works on glass alteration it was determined that alkalis (Na, K), acting as modifiers of the glassy network, are damageable to glass durability, hence the development of surface treatments willing to deplete glass surfaces in alkalis prior to their normal use, like observed for SO<sub>2</sub> dealkalization treatments. It was highlighted in this work that these surface treatments were found to efficiently reduce the leaching of elements like Pb over long periods of time, but also Ba by modifying their release mechanism and making the ion-exchange and interdiffusion component of alteration almost undetectable. On treated samples (CEMa and CEMb) the release of Pb and Ba appeared driven by the hydrolysis of the surrounding silicate network, which depends on experimental parameters like temperature, pH and SA/V ratio. However, for glasses normally not subjected to interdiffusion like low alkalis borosilicate glasses, SO<sub>2</sub> dealkalization treatments were found useless. The acid etching conventionally used by glassmakers for aesthetic purposes, was found to have a non-existent to detrimental effect on glass durability and the retention of Pb, Ba and B. However, in the case of opal-crystallized glass plates, the abrasion of the vitreous air-exposed surface resulted in a more durable glass surface, reinforced by the presence of crystals. Surface coatings of silicon oxide and tin oxide were found to be rapidly hydrolysed in the leaching process poorly impacting glass durability on the long run, except for Pb on lead crystal glasses where distinctive reduction of lead release was noticed. Nonetheless, the net surface modifications induced by these very thin layers (10 nm) were evidenced and could imply major changes for thicker coatings. Regarding titanium oxide coating, its use raises concerns in terms of ecotoxicity, but its retention towards boron remained the most efficient of

our panel although the diffusion and retention capacities of these durable titanium oxide layers were not elucidated.

## Methods

### Sample preparation

Glass items were retrieved from industrial production lines before any surface treatment was applied. These were then annealed to be cut into glass slabs of approximately 2 × 2 cm<sup>2</sup>. For glasses B and O, the items were 4 mm thick glass plates and the original surfaces of the top and bottom were conserved to make our experiments true to real case usage of these items. Consequently, the slabs cut from these items exhibited a ruguous phase corresponding to the glass in contact with the steel mould in which they were shaped on the other side a very smooth large face referred to as the air side. In this case the rugosity originates from the moulding of the plate and did not generate glass constraints.

The square shaped glass slabs were then sent to industrial manufacturers to apply the surface treatments. The received treated and non-treated glass samples were then quickly washed with ethanol and then acetone before starting the leaching tests and pristine glass characterizations.

### Surface treatments

Acid etching consists in alternating baths of highly concentrated hydrofluoric and sulphuric acids. Surface dealkalization by SO<sub>2</sub> vapour treatment consists in heating a sulphur-bearing precursor to create gaseous SO<sub>2</sub> which reacts with the alkalis at the glass surface below the glass annealing temperature to form sodium sulphate precipitates. These latter are washed out using weakly acidic solution and the resulting glass surface are dealkalized, superficially impoverished in Na and K. For coating surface (SiO<sub>2</sub>, SnO<sub>2</sub> and TiO<sub>2</sub>), the glass items are treated using Chemical Vapour Deposition (CVD) process before entering the annealing arch at temperatures over 450 °C.

### Leaching experiments

Long term alteration tests in static mode were performed in perfluoroalkoxy alkane reactors (PFA), at 70 ± 3 °C in 4% vol. acetic acid solution, which corresponds to a pH of 2.4 ± 0.1. The acetic acid 4% vol. solution was prepared by diluting acetic acid (100%, Merck Suprapur) in 18 MΩ.cm ultrapure water. Each of the 35 different samples listed in Table 2 was leached in an individual container with one glass slab per reactor, elevated by a sample holder made of PFA to maximize contacts between the glass slab and the alteration solution. The initial glass- surface-area-to-solution-volume-ratio (SA/V) was determined by precisely measuring the length, width and height of each glass slab using a digital caliper (with 0.01 mm uncertainty accounting for instrumental and experimental error) and the volume of solution was calculated from the mass of solution introduced in the reactor. The initial SA/V ratio varied between 2.36 and 2.52 m<sup>-1</sup>. Regularly, small volumes (≤3 mL) of alteration solution were sampled from each reactor to be analysed by ICP-MS. The total volume of solution sampled from each reactor did not exceed 10% of the initial total volume of solution and the SA/V ratio was recalculated after each sampling to take into account the evolution of the volume of solution. Alteration was carried out for 470 days (1.3 years) except in some cases, where evaporation caused a significant reduction of the volume of solution of alteration requiring to stop and dismantling these reactors prematurely. After alteration, all the glass slabs were removed from the reactors and dried at 70 °C for 2 h before cooling down overnight at room temperature and humidity. The dry and altered slab was then cut in two to four pieces to allow different types of characterization. Since the surface of the glass slab after chemical deposit or chemical attack was modified and did not correspond to the bulk glass composition anymore, it is not possible to calculate normalized loss nor equivalent thickness of glass altered which are indicators of the glass alteration based on the glass composition and usually used among the glass alteration community. Nonetheless the alteration was quantified by determining in each sample of the glass alteration solution the total element concentrations using a quadrupole inductively coupled plasma-mass spectrometer (ICP-MS, Agilent 7900) after dilution 1/10 with HNO<sub>3</sub>



0.5 N. These elemental concentrations were then normalized to the SA/V ratio after taking in consideration the dilution factor determined by recording the mass of samples before and after dilution with a 0.0001 g precision balance.

$$SA/V_{geo} = \frac{A}{V_{sol}} \quad (1)$$

With SA/V the glass-surface-area-to-solution-volume-ratio ( $m^{-1}$ ), determined from  $V_{sol}$  the volume of solution in the experiment ( $m^3$ ),  $A$  the area of the glass slab in contact with the alteration solution ( $m^2$ ).

For this protocol, relative uncertainties were calculated based on the standard deviation yielded from the ICP-MS determination of the concentrations in solution, which is the main factor contributing for the experimental and instrumental uncertainties.

### ToF-SIMS

Depth profiles were analysed on the smooth face of the pristine and altered glass slabs by Time of Flight-Secondary Ion Mass Spectroscopy (ToF-SIMS) with an IONTOF TOF 5 instrument at Tescan Analytics (France) using  $O^{2+}$  sputtering and  $Bi^+$  analyzing beams scanning a surface-area of  $50 \times 50 \mu m^2$ . Oxygen beam was tuned at 0.5–2 keV and 75–250 nA depending on the targeted depth of analysis. Only positive mode was used. The depth of the craters was measured after the analyses using a mechanical profilometer and profiles were calculated assuming that the sputtering rate was constant. Regarding data processing, for each mass spectrum recorded, the intensity of each element was normalized to the total intensity accounting for all the ions collected to rectify any fluctuation of the signal caused by variations from the ion source, as shown in Eq. (2). Then, the profiles of interest were normalized to the mean value obtained in the pristine glass with Eq. (3) to cut off the signal of the pristine glass and evaluate the relative behaviour of each element in the altered glass. All elements profiles are thus set to 1 in the pristine glass.

$$J_i = \frac{A_i}{A_{tot}} \quad (2)$$

With  $J_i$  the intensity of element  $i$  normalized to the total count of ions,  $A_i$  the intensity of element  $i$  and  $A_{tot}$  the total intensity collected on the mass spectrometer.

$$J_{norm_i} = \frac{J_i}{\frac{1}{n_{sup} - n_{inf}} \sum n_{inf}^i} \quad (3)$$

With  $J_{norm_i}$  the intensity of element  $i$  normalized to the pristine glass,  $J_i$  the intensity of element  $i$  normalized to the total count of ions,  $n_{inf}$  corresponding to the index of the first point considered as pristine glass,  $n_{sup}$  corresponding to the index of the last point in the profile.

Please note that the ionic form exhibited in the figure's legend or in the text do not represent the ionization of the elements in the sample but the species detected by the secondary ion mass spectrometer after sputtering.

### Scanning electron microscopy

The morphology of the pristine and altered glass slabs was examined by field emission gun-scanning electron microscopy (FEG-SEM) using a Zeiss Supra 55 at 15 kV (probe current about 1 nA). To allow precise mapping, the samples were embedded in an epoxy resin and polished before coating with a 15 nm carbon layer for electronic conduction. The determination of the chemical distribution of the different elements within the samples was obtained from energy dispersive X-ray spectroscopy (EDS) analyses on plane polished samples with a Bruker AXS X-FlashDetector 4010 system. Data collection and treatment were done with the ESPRIT2.0 software (Bruker<sup>TM</sup>, USA).

### Data availability

The data that supports the findings of this study are available from the corresponding author upon reasonable request.

Received: 24 August 2023; Accepted: 10 October 2024;

Published online: 26 October 2024

### References

- Hartmann, P., Jedamzik, R., Reichel, S. & Schreder, B. Optical glass and glass ceramic historical aspects and recent developments: a Schott view. *Appl. Opt.* **49**, D157 (2010).
- Alloteau, F. et al. Study of a surface treatment based on zinc salts to protect glasses from atmospheric alteration: Mechanisms and application to ancient glass objects in museum. In *Glass atmospheric alteration: cultural heritage, industrial and nuclear glasses*. Hermann Ed., Paris, 2019.
- E.U. Council Directive of 15 December 1969 on the approximation of the laws of the Member States relating to crystal glass, December 1969. URL <https://eur-lex.europa.eu/legal-content/EN/ALL/?uri=celex:31969L0493>.
- Graziano, J. H. & Blum, C. Lead-exposure from lead crystal. *Lancet*, **337**, 141–142, (1991).
- Susan, C. Hight. Lead migration from lead crystal wine glasses. *Food Addit. Contam.* **13**, 747–765, (1996).
- Bonnet, C. et al. Alteration of lead silicate glasses due to leaching in heated acid solutions. *J. Non Crystalline Solids* **323**, 214–220, (2003). ISSN 0022-3093URL.
- Sadrnezhaad, S. K., Rahimi, R. A., Raisali, G. & Foruzanfar, F. Mechanism of deleading of silicate glass by 0.5N HNO<sub>3</sub>. *J. Non Crystalline Solids* **355**, 2400–2404 (2009).
- Ali Rahimi, R. & Sadrnezhaad, S. K. Effects of ion-exchange and hydrolysis mechanisms on lead silicate glass corrosion. *Corrosion* **68**, 793–800 (2012).
- van Elteren, J. T., Grilc, M., Beeston, M. P., Reig, M. B. & Grgic, I. An integrated experimental-modeling approach to study the acid leaching behavior of lead from sub-micrometer lead silicate glass particles. *J. Hazard. Mater.* **262**, 240–249 (2013).
- Angeli, F., Jollivet, P., Charpentier, T., Fournier, M. & Gin, S. Structure and chemical durability of lead crystal glass. *Environ. Sci. Technol.* **50**, 11549–11558 (2016).
- Brunswic, L. et al. Comparative study of the structure and durability of commercial silicate glasses for food consumption and cosmetic packaging. *npj Mater. Degrad.* **8**, 82 (2024).
- Kravchenko, J., Darrah, T. H., Miller, R. K., Lyster, H. K. & Vengosh, A. A review of the health impacts of barium from natural and anthropogenic exposure. *Environ. Geochem. Health* **36**, 797–814 (2014).
- ISO 7086-1:2019. Glass hollowware in contact with food - Release of lead and cadmium. Part 1 : test method (2019).
- Graziano, J. H., Slavkovic, V. & Blum, C. Lead crystal: an important potential source of lead exposure. *Chem. Speciat. Bioavailab.* **3**, 81–85 (1991).
- Guadagnino, E., Gramiccioni, L., Denaro, M. & Baldini, M. Co-operative study on the release of lead from crystalware. *Packag. Technol. Sci.* **11**, 45–57 (1998).
- Senturk, U., Vamer, J. R. & LaCourse, W. C. Structure-hardness relation for high- temperature SO<sub>2</sub>-dealkalized float glass. *J. Non-Crystalline Solids* **222**, 160–166 (1997).
- Sheth, N., Luo, J., Banerjee, J., Pantano, C. G. & Kim, S. H. Characterization of surface structures of dealkalized soda lime silica glass using X-ray photoelectron, specular reflection infrared, attenuated total reflection infrared and sum frequency generation spectroscopies. *J. Non-Crystalline Solids* **474**, 24–31 (2017).
- Sheth, N. et al. Effects of acid leaching treatment of soda-lime silicate glass on crack initiation and fracture. *J. Am. Ceram. Soc.* **104**, 4550–4558 (2021).



19. Lecanuet, G., Rocca, E., Hee, P., Skaper, M. A. & Rapin, C. Mechanism of alteration of the surface of lead crystal glass in contact with food: a chemical study of the surface layer. *Appl. Surf. Sci.* **580**, 152281 (2022).
20. E.U. Commission Delegated Regulation (EU) 2021/849 of 11 March 2021 amending, for the purposes of its adaptation to technical and scientific progress, Part 3 of Annex VI to Regulation (EC) No 1272/2008 of the European Parliament and of the Council on classification, labelling and packaging of substances and mixtures, May 2021.
21. Tricot, G. The structure of Pyrex® glass investigated by correlation NMR spectroscopy. *Phys. Chem. Chem. Phys.* **18**, 26764–26770 (2016).
22. Perera, G. & Doremus, R. H. Dissolution rates of commercial soda-lime and pyrex borosilicate glasses: influence of solution pH. *J. Am. Ceram. Soc.* **74**, 1554–1558 (1991).

### Acknowledgements

This study was supported by the French Agency for Research (ANR, PRCE program, grant 18-CE08-0025). Prime Verre prepared the glass slabs. Elodie Chauvet, Loan Lai, Florian Cousy and Yves Depuydt from Tescan Analytics performed the ToF-SIMS profiles. Filab analysed the glass compositions. ICP-MS analyses were partly supported by the IPGP multi-disciplinary program PARI and by Paris-IdF region SESAME Grant no. 12015908.

### Author contributions

L.B. performed the leaching experiments, L.B. carried out the SEM and ToF-SIMS observations and all the data curation. Ev.H. ran the elemental analyses by ICP-MS. F.A., S.G. and L.B. supervised the study and worked on the conceptualization, methodology and original draft. All the authors helped on the paper editing.

### Competing interests

The authors declare no competing interests.

### Additional information

**Supplementary information** The online version contains supplementary material available at <https://doi.org/10.1038/s41529-024-00526-x>.

**Correspondence** and requests for materials should be addressed to F. Angeli.

**Reprints and permissions information** is available at <http://www.nature.com/reprints>

**Publisher's note** Springer Nature remains neutral with regard to jurisdictional claims in published maps and institutional affiliations.

**Open Access** This article is licensed under a Creative Commons Attribution 4.0 International License, which permits use, sharing, adaptation, distribution and reproduction in any medium or format, as long as you give appropriate credit to the original author(s) and the source, provide a link to the Creative Commons licence, and indicate if changes were made. The images or other third party material in this article are included in the article's Creative Commons licence, unless indicated otherwise in a credit line to the material. If material is not included in the article's Creative Commons licence and your intended use is not permitted by statutory regulation or exceeds the permitted use, you will need to obtain permission directly from the copyright holder. To view a copy of this licence, visit <http://creativecommons.org/licenses/by/4.0/>.

© The Author(s) 2024